Korean J. Chem. Eng., **28**(6), 1406-1411 (2011)
DOI: 10.1007/s11814-010-0508-9

Therapeutic effect of chitosan modification on salmon-calcitonin-loaded PLGA nanoparticles

Min-Jeong Lee*, Da-Young Seo*, Hea-Eun Lee, and Guang Jin Choi*,**,†**

*Department of Smart Foods and Drugs, and **Department of Pharmaceutical Engineering,
Inje University, Gimhae, Gyeongnam 621-749, Korea
(*Received 5 October 2010 • accepted 4 December 2010*)

Abstract−Although salmon-calcitonin (sCT) has been known as a potent drug for the treatment of osteoporosis, its oral dosage form products have not been commercially available primarily due to a poor oral bioavailability. Chitosan has been extensively examined as a potential oral absorption enhancer, whereas encapsulation with PLGA has been widely studied to address the delivery problems of typical peptide drug molecules. We investigated the mechanism and therapeutic effect of chitosan modification on the sCT-loaded PLGA nanoparticles. Chitosan was added onto these particles in two ways: by incorporation during W/O/W emulsification and by solid dipping. Particles were characterized by particle size analyzer, Zeta potential analyzer, scanning electron microscopy, and so forth. Nano-sized particles of 430-590 nm in fairly spherical shape with a narrow size distribution were produced. The PLGA encapsulation efficiency greater than 50% of added sCT was achieved regardless of chitosan modification. It turned out that sCT-loaded PLGA particles with chitosan modified during W/O/W emulsification (referred to as sCT-PLGA-CHT1) showed better therapeutic behavior in terms of sustained release effects as well as short-period hypocalcemic effects than the others. It was concluded that the beneficial effect was greatly associated with the formation of embedded structure of chitosan molecules when particles were modified with chitosan.

Key words: Salmon-calcitonin (sCT), Chitosan, PLGA, Hypocalcemic Effect, Oral Absorption

INTRODUCTION

Chitosan-based controlled delivery systems were described to have unique polymeric character, gel-forming properties and propensity to degradation [1]. The positive effect of chitosan on the transmucosal delivery of peptides and proteins has been explained by its mucoadhesive properties and its capacity to open tight junctions between epithelial cells, thus facilitating the transport of macromolecular drug through well-organized epithelia [2]. The effect of chitosan added in two types to the sCT solution on in vivo nasal absorption in rats was investigated [3]. The bioavailability was increased up to 1.25% of sCT content in terms of safety and effectiveness. Nevertheless, the bioavailability of nasal administration by chitosan addition was about 2.5% at maximum compared to IV. Heparin was encapsulated with chitosan and chondroitin sulfate complex by emulsion-chemical crosslink method [4].

According to IR, SEM, and thermal analysis, there were electrostatic interactions between the amino groups of chitosan and the sulfate group and free carboxyl group, which protected the drug and adjusted its release rate depending upon the pH. Chitosan was used to prepare composite microparticles with alginate and pectin to delivery bovine serum albumin [5]. It was reported that composite microparticles (less than 200 μm) with suitable chitosan composition showed effectively sustained BSA release at pH 1.2 and pH 5.0. On the other hand, at neutral pH, the drug release was increased significantly.

†To whom correspondence should be addressed.
E-mail: pegchoi@inje.ac.kr

Drug-loaded PLGA particulate systems combined with chitosan coating have been very extensively studied. Chitosan-modified eCT-loaded PLGA nanoparticles were prepared by emulsion solvent diffusion and nebulized for a pulmonary delivery [6]. According to a chitosan-coated PLGA nanoparticle study, the particle size and surface charge were the most significant determinants in the cellular uptake and trafficking of nanoparticles [7]. Chitosan-coated PLGA particles which were prepared by the emulsion-diffusion-evaporation technique effectively bound antisense RNAs and were taken up into cells. Chitosan-coated PLGA nanoparticles prepared by emulsion solvent diffusion (ESD) method were investigated for gene delivery [8]. Instead of bioadhesion, a chitosan coating resulted in an increase in gen loading efficiency. Besides, the initial burst of nucleic acids was significantly alleviated, which would favor sustained release.

Chitosan-modified paclitaxel-loaded PLGA nanoparticles (200-300 nm) were prepared by a solvent evaporation method to examine their lung-specificity [9]. When they were administered intravenously, transient aggregates were formed in the bloodstream due to chitosan-related interactions, which presumably resulted in an enhanced trapping of nanoparticles in the lung capillary responsible for the lung-tumor-specific distribution. Zeta potential and in vitro cellular cytotoxicity of above nanoparticles were examined as the medium pH varied 6.8-8.0 [10]. It was concluded that enhanced electrostatic interactions between chitosan modified surface of nanoparticles and acidic microenvironment of tumor cells played an important role in lung-tumor specific accumulation of chitosan-modified paclitaxel-loaded PLGA nanoparticles.

Alveola-targeted rifampicin-loaded microparticles were studied as to their encapsulation and nebulization behaviors with respect to

chitosan addition [11-13]. Overall, the incorporation of chitosan in a suitable level to PLGA resulted in a formation of very stable microparticles with high drug loading capacity, lower cytotoxicity towards alveolar epithelial cells (compared to PLGA particles) and equivalent (with chitosan particles) mucoadhesive properties [11]. But in some cases, the reverse is true. A study on chitosan-coated PLGA micrsoparticles leaded with rifampicin revealed an increased burst release compared to uncoated PLGA particles, probably attributed to the higher solubility of chitosan in acidic media [12]. Nevertheless, the drug-leading ability and the nebulation stability were substantially enhanced by chitosan-coating. In a continuing study, the effect of chitosan coating on encapsulation efficiency, nebulization efficiency, and stability of rifampicin-loaded liposomes were examined with various surface charge states [13]. Negatively-charged liposomes were coated by chitosan better, which gave a significant improvement in nebulization behavior while the gain in the encapsulation efficiency was marginal.

In contrast to PEG coating, chitosan-coated lipid particles loaded with a drug were able to open the tight junction by favorable interactions, thereby increasing the permeability of the Caco-2 model epithelium [14]. Moreover, chitosan-coated nanoparticles enhanced the oral absorption of peptide sCT leading to a prolonged hypocalcemic response. The effect of chitosan coating to γ-oryzanol-loaded calcium pectinate on the release pattern was studied [15]. Ca pectinate, well explained as 'egg-box model' by ionotropic gelation with divalent Ca^{2+} ion, has been widely used for oral drug delivery. It was concluded that the drug release was efficiently suppressed by a chitosan coating in both gastric fluid and intestinal fluid. Tamoxifen-loaded crosslinked alginate microparticles for targeting Peyer's patch uptake were coated by chitosan [16].

The absorption enhancing effect of chitosan has attracted much more attention recently for various administration routes. Nevertheless, little has been reported regarding the beneficial effect and mechanism of chitosan coating on the improved oral absorption of sCT toward the treatment of osteoporosis. In our previous study, sCT-loaded PLGA nanoparticles were prepared by W/O/W emulsification and evaporation and examined for oral delivery capability [17]. Encapsulation efficiencies of greater than 50% along with improved oral absorption were achieved. Also, we reported that the oral absorption of sCT-loaded PLGA nanoparticles was enhanced by adding a moderate amount of bile acid [18].

In this study, sCT-loaded PLGA nanoparticles modified with chitosan in a novel method were tested for an improved hypocalcemic effects. The mechanism and the therapeutic effect of the chitosan modification were examined along with the physicochemical properties and *in vivo* behavior of sCT-loaded PLGA particles.

EXPERIMENTAL SECTION

1. Materials

Salmon calcitonin (sCT) was purchased from Bachem AG (Bubendorf, Switzerland). D,L-lactide-co-glycolide polymers (PLGA) of 50 : 50 molar ratio (Resomer RG503H, MW 40,000-75,000) and Polyvinylalcohol (PVA, MW 86,000, 99-100% hydrolyzed form) were supplied by Boehringer Ingelheim (Ingelheim, Germany) and ACROS (New Jersey, USA), respectively. Chitosan (MW 190-310 kDa, 75-85% of deacetylation degree, viscosity 200-800 cP at 1% in 1% acetic acid) was bought from Sigma-Aldrich (St. Louis, USA). All other reagents used in this study were of reagent grade.

2. Preparation of Chitosan-modified sCT-loaded PLGA Nanoparticles

Fig. 1 illustrates a schematic diagram to prepare medicated par-

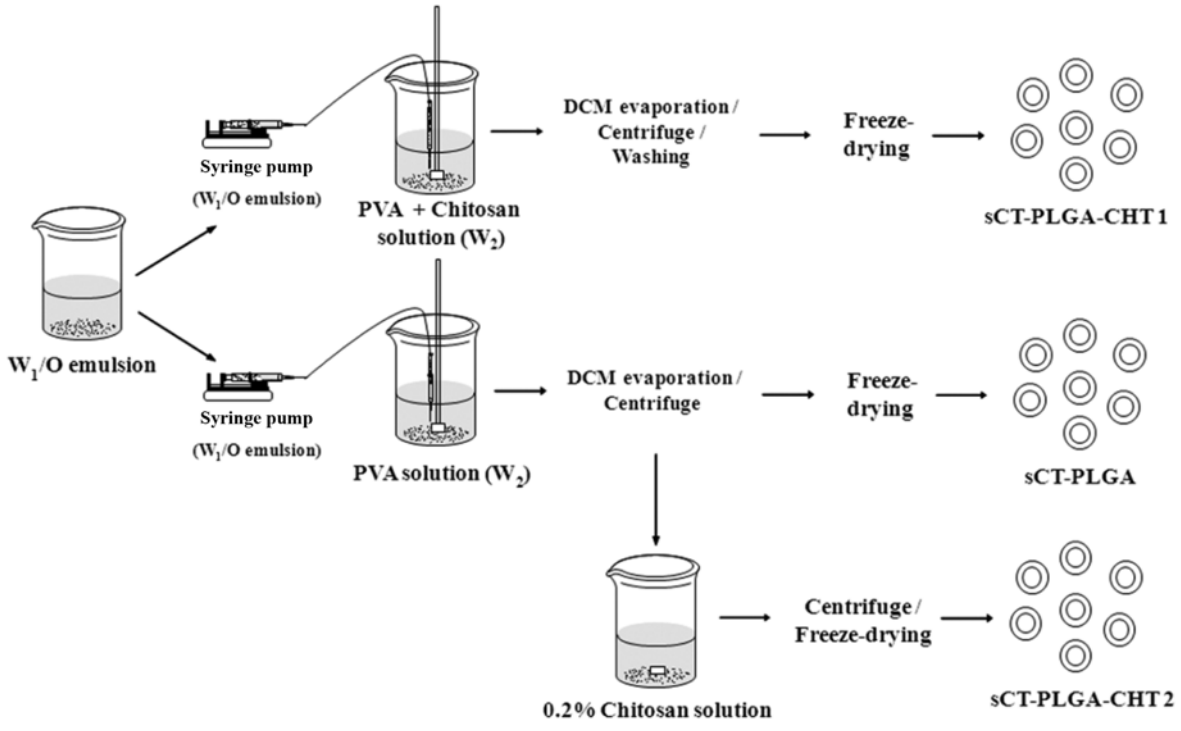

Fig. 1. Schematic diagram of medicated nanoparticle preparations.

ticles. sCT-loaded PLGA nanoparticles were prepared using $W_1/O/W_2$ double emulsion-solvent evaporation method as described in detail elsewhere [17]. In brief, 10 mg of sCT was dissolved in 1 mL of de-ionized water (W_1). PLGA of 300 mg was dissolved in 20 mL methylene chloride (O) which contained 100 μL of polysorbate-20. These W_1 and O phases were mixed together and homogenized at 13,000 rpm for 1 min using the ULTRA-TURRAX mixer (T25, IKA, Germany) to form a primary W_1/O emulsion. The emulsion was injected into 200 mL of 1% (w/v) PVA solution (W_2) under a vigorous agitation using a peristaltic syringe pump (KDS 100, Kd Scientific, USA) followed by a homogenization at 5,200 rpm for 30 min.

The methylene chloride was removed from the emulsion by using an evaporator (Bchi R-210, Switzerland) prior to being stored at 4 °C for 24 h. The final emulsion-derived suspension was centrifuged (Combi-514R, Hanil Science Ind., Korea) at 13,000 rpm for 30 min to collect the sCT-loaded PLGA nanoparticles. The sediment was rinsed twice with DI water and freeze-dried (Cleanvac 8, BioTron, Korea) overnight.

Chitosan-modified sCT-loaded PLGA nanoparticles were prepared by two different methods. Firstly, 50 mL of 1% (w/v) chitosan solution was added to the 1% (w/v) PVA solution (200 mL) to make W_2 phase (referred to as sCT-PLGA-CHT1). Therefore, chitosan was included in W/O/W emulsion as an ingredient of W_2 before undergoing evaporation and centrifugation. Secondly, the suspension comprising sCT-loaded PLGA nanoparticles after water-rinsing step and ensuing centrifugation was added to a 0.2% (w/v) chitosan solution (50 mL) followed by 30 min stirring (referred to as sCT-PLGA-CHT2). For a comparison, a higher chitosan content (1%) solution was used for the second method. Since the chitosan was not well soluble in DI water, it was dissolved in 1% (v/v) acetic acid. Viscosities of emulsification solutions were measured with a viscometer (Brookfield DV-I+, Middleboro, USA). All other procedures except the surface modification step were exactly the same as mentioned previously.

3. Measurement of Encapsulation Efficiency of sCT

The encapsulation efficiency (EE) of sCT in nanoparticles was determined by measuring the amount of free-sCT in the supernatant that resulted from the centrifugation and rinsing steps. The BCA (bicinchoninic acid) protein assay [19] was used to evaluate the amount of free-sCT and the absorbance was measured with UV-visible spectrometer (UV-160 PC, Shimadzu, Japan). All samples were analyzed in triplicate and EE (%) of sCT was calculated using the equation below:

$$\text{E.E. } (\%) = \frac{\text{total sCT amount} - \text{free sCT amount}}{\text{total sCT amount}} \times 100$$

4. Measurements of Particle Size Distribution and Surface Charge (by Zeta-potential)

A particle size analyzer (90PLUS, BIC, USA) was used to measure the particle size and its distribution presented as polydispersity index (PI). Each particle specimen was suspended in DI water. Span 80 (Samchun Pure Chem., Korea) was added as a surfactant to make 0.01% (v/v). Sonication was performed for 5 min prior to every PSA measurement.

Zeta-potential analyzer (ELS-8000, Otsuka Electronics, Japan) was employed to estimate quantitatively the degree of surface modification by chitosan onto sCT-loaded PLGA nanoparticles. For this objective, chitosan-modified particles in various formulations (including no chitosan) as well as pure chitosan particles were measured for zeta potential values. The solid content for each sample was settled to be 1 μg/mL.

In addition, particles in various formulations were measured for surface morphology by scanning electron microscopy (SEM; S4300-SE, Hitachi, Japan). To minimize the detrimental effect of electron beam on polymeric particle specimens, each SEM measurement was performed on a cryogenic stage.

5. *In Vivo* Study

All the animal procedures were performed in accordance with NIH Guidelines for Animal Care and Use, and the experimental protocols were reviewed and approved by the Inje University Animal Care and Use Committee at Inje University Animal Resource Center. Sprague-Dawley (S.D) male rats of seven weeks old and 240-260 grams (Samtako Bio, Korea) were employed for the *in vivo* oral absorption study. For each rat, a venous catheter was installed into the jugular vein near the jaw bone with urethane anesthesia of abdominal cavity. *In vivo* experiment was performed after each catheter-installed S.D rat went through 3 day convalescence period, fed with potable water only. Medicated particles in various formulations were orally administered to the rats classified in four different groups. For each group, five S.D rats were examined. As-purchased sCT and sCT-PLGA particles at 500 IU/kg dispersed in saline solution were administered to group 1 and group 2, respectively. The sCT-PLGA-CHT1 and sCT-PLGA-CHT2 particles were administered under the same condition to group 3 and 4, respectively. For comparison, the saline solution alone was administered to the control group.

The blood drawn right after a strength recovery prior to drug administration was used as a standard data. Then, various formulations including the solely saline solution were administered to those rats. After drug administration, 300 mL of blood was drawn from each test rat at the following time marks: 0, 6, 14, 30, 60, 120, 180, 240, 300, 360, 420, 720 min. Collected blood was centrifuged using a high-speed centrifuge (5417R, Eppendorf AG, Germany) under a predetermined condition (at 10,000 rpm and 4 °C for 5 min). The plasma was extracted from centrifuged substances and stored in a deep-freezer (at −80 °C) until its analysis.

6. Analysis of Blood Ca^{2+} Concentration

Plasma of 10 mL extracted from each rat was positioned as droplets on the Ca^{2+} kit (Fuji Dry-Chem Slide Ca-PIII, Fuji Photo Film, Japan) and measured using an automatic dry chemistry analyzer for veterinary (Fuji Dry-Chem 3500i, Fuji Photo Film, Japan). The photometry method has been extensively employed to measure the absorbance of chelate produced by combining calcium ion with dyes such as glyoxal-bis (2-hydroxyanil), alizarin, chlorophosphonazo III, methylthymol blue, o-cresolphthalein complexone and arsenazo III. In our study, the calcium ion in each kit was combined with chlorophosphonazo III [20].

7. Statistical Analysis

All values were expressed as the mean±standard deviation (SD). Comparisons among groups were made by one-way analysis of variance (ANOVA) and Student-Newman-Keuls (SNK) test using SigmaStat software, version 3.0 (Systat Software Inc., USA). Differences were considered to be significant at a level of $P<0.05$.

RESULTS AND DISCUSSION

1. Characteristics of Chitosan-modified Nanoparticles

As mentioned previously, there are three classes of nanoparticles: sCT-PLGA, sCT-PLGA-CHT1, sCT-PLGA-CHT2. Fig. 2 compares their SEM images. In all cases, the nanoparticles showed spherical shape regardless of the designation. Therefore, the addition of chitosan to PLGA particles did not cause any appreciable change in surface morphology. It means that the beneficial action of a chitosan modification, if any, for an enhanced oral absorption would not be primarily associated with a physical effect such as mechanical interlocking.

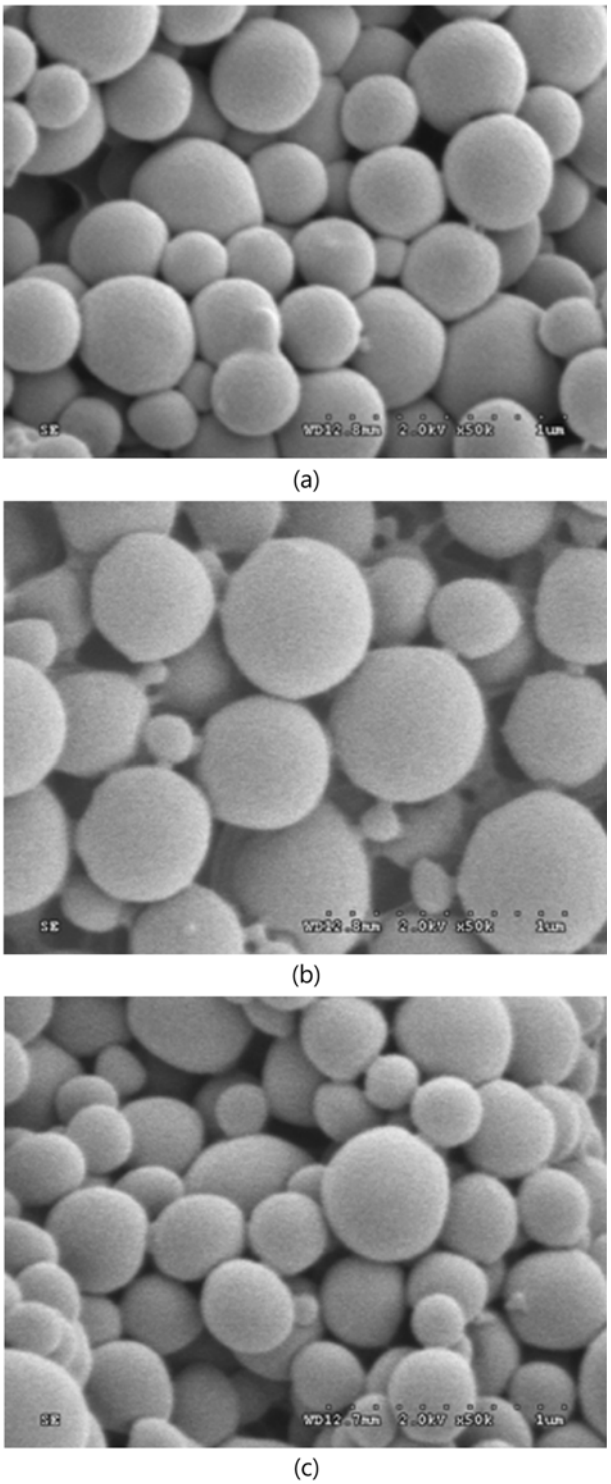

Fig. 2. SEM micrographs: (a) sCT-PLGA, (b) sCT-PLGA-CHT1, and (c) sCT-PLGA-CHT2 nanoparticles.

On the other hand, there was significant difference in the particle size determined by SEM. The PSA results confirmed this observation. As shown in Table 1, mean diameters of sCT-PLGA, sCT-PLGA-CHT1 and sCT-PLGA-CHT2 were 443.1±23.6 nm, 588.9±22.8 nm and 429.7±13.1 nm, respectively. Each value was calculated from the results of triplicate experiments. Since the standard deviation for each particle class was fairly small, these nanoparticles are presumed to have narrow size distribution.

The zeta potential was measured to observe the surface charge state of various nanoparticles. The zeta potential value of pure chitosan particles as s reference point was 9.89±0.21 mV. The positive surface potential was expected because chitosan would be ionized to make $-NH_3^+$ ion under appropriate condition. The sCT-PLGA particles gave −8.83±0.25 mV representing a negative surface charge as anticipated from a dissociation of carboxylic acid functionality in PLA and PGA.

On the other hand, as shown in Table 1, both chitosan-modified sCT-loaded PLGA nanoparticles gave positive zeta-potential values. Since the zeta-potential values of both chitosan-modified particles are substantially different from that of sCT-PLGA particles, it is clear that both particles were well covered by chitosan on their outer surfaces. In principle, as particles are modified more with chitosan, their surface characteristics would turn more like that of chitosan molecules.

There was a noticeable difference in the mean diameter between sCT-PLGA-CHT1 and sCT-PLGA-CHT2 particles (see Table 1). The mean diameter of sCT-PLGA-CHT2 particles was very close to that of sCT-PLGA, which was anticipated because an additional coating on sCT-PLGA particles would not increase their final diameter significantly. The mean diameter of sCT-PLGA-CHT1, however, was measured to be substantially greater than the others.

This result might be caused by the difference in the solution viscosity of W_2 phase. The dynamic viscosities of 1% PVA solution and 1% chitosan solution were 4.5 cP and 373.2 cP measured at 22 °C and 100 rpm for 1 min, respectively. Therefore, the chitosan solution was much more viscous than the PVA solution. The viscosity of the mixture solution for W_2 phase was 30.0 cP. Since the W_1/O emulsion was homogenized in a more viscous chitosan-containing W_2 phase to make W/O/W emulsion, the chopping action to small emulsion particles would have been hindered to a greater extent. Accordingly the W/O emulsion was poorly homogenized to lead to sCT-PLGA-CHT1 particles larger than others.

2. Effect of Chitosan Modification on Encapsulation Efficiency

The encapsulation efficiency (EE) of sCT was measured by using BCA protein assay. This analysis method is to use color reaction of complex formed by bicinchonic acid (BCA) and Cu^{2+}. The complex of madder lake is measured for absorbance at wavelength of 562 nm. The BCA protein assay reactions are known as follows:

1. protein+Cu^{2+}+OH^- → Cu^+
2. Cu^++2 BCA → Cu^+/ BCA chromophore (at 562 nm)

Table 1. Comparison of the zeta-potential and particle size of various nanoparticles

Item	sCT	sCT-PLGA	sCT-PLGA-CHT1	sCT-PLGA-CHT2 (0.2% CHT)
Particle size (nm)	655.7±20.1	443.1±23.6	588.9±18.8	429.7±13.1
Polydispersity	-	0.177±0.034	0.279±0.023	0.251±0.025
Zeta potential (mV)	9.89±0.21	−8.83±0.25	5.72±1.04	7.63±0.93

Table 2. Encapsulation efficiency (EE) of various nanoparticles

Item	sCT-PLGA	sCT-PLGA-CHT1	sCT-PLGA-CHT2		
			Before coating	After coating (0.2% CHT)	After coating (1% CHT)
EE (%) Mean	54.2±3.9	54.2±4.6	50.9±2.6	49.6±4.5	36.4±4.1

The measured EE values of various nanoparticles are summarized in Table 2. The values in the table were calculated from the results of triplicate batch preparations. Above all, as seen in the table, the reproducibility seemed very good. There was no appreciable difference in EE value between sCT-PLGA and sCT-PLGA-CHT1 particles, whose EE values ranged 53-56%. There have not been many cases reported where EE values for sCT encapsulation with PLGA greater than 50% were achieved. Hence, during the second emulsification in W_2 phase that included PVA and chitosan, sCT did not diffuse out of O phase appreciably.

For sCT-PLGA-CHT2 particles, three EE values were measured: before coating, and after coatings in 0.2% and 1% chitosan solutions. Before the chitosan coating, the EE value was about 51%, very comparable to that of previous two nanoparticles. A coating in 0.2% chitosan solution that is very similar to the W_2 solution for sCT-PLGA-CHT1 particles gave about 50%, basically the same value as above. The coating in 1% chitosan solution, however, resulted in decreased EE values around 36%.

Our speculation for this distinct loss in EE is as follows. When sCT-loaded PLGA particles were dipped in a chitosan solution, molecular diffusion in both directions would take place, that is, chitosan into PLGA particle and sCT out of PLGA particles. The pH values of 0.2% and 1% chitosan solutions were 4.3 and 3.5, respectively. Since the pI (isoelectric point) of sCT is reportedly 10.4, sCT is regarded as weakly basic. Accordingly, the diffusion of sCT molecules through the solid PLGA wall would be significantly affected by the pH of the surrounding solution. In 1% chitosan solution whose pH was 3.5, sCT was more likely to move out of the PLGA nanoparticles into the surrounding chitosan solution compared to the dip-coating in 0.2% chitosan solution. It also explains why the EE value of sCT-PLGA-CHT1 particles was kept above 50%. Although not performed, a W/O/W emulsification in a more acidic solution would have resulted in a significant loss in the sCT retention of PLGA nanoparticles.

When we measured the chitosan contents in these two particles via FT-IR and HPLC, no appreciable difference was observed. Now, an interesting issue is why there was some difference in zeta potential (see Table 1) between sCT-PLGA-CHT1 and sCT-PLGA-CHT2 particles if the chitosan content was about the same. This difference would be associated with the spatial distribution of chitosan molecules throughout the sCT-loaded PLGA particles. For sCT-PLGA-CHT2 particles, chitosan would exist mostly on the outermost surface. On the other hand, chitosan molecules seemed to be partly embedded in the sCT-PLGA-CHT1 particles. As a result, some chitosan molecules embedded deep enough in PLGA matrix were not seen by the zeta potential measurement, which gave a lower positive value as zeta potential. This difference in the spatial distribution of chitosan was related to *in vivo* results as well.

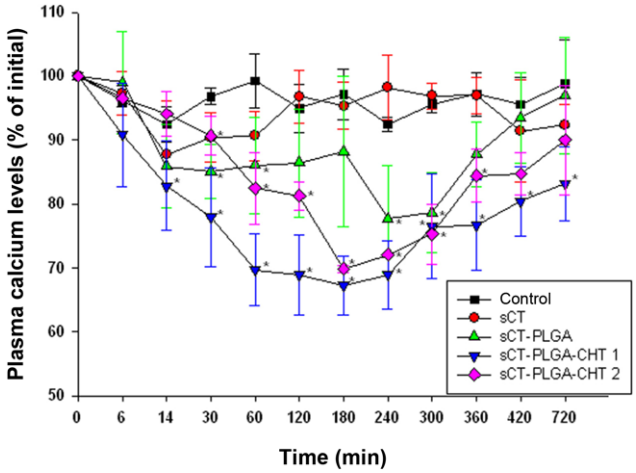

Fig. 3. Comparison of hypocalcemic effects of various nanoparticles with respect to time (Each data point represents the mean±SD @ n=5) (* indicate significant differences compared to the control (p<0.05)).

3. *In Vivo* Study

In-vivo study was performed with five groups, five S.D male rats for each group. Fig. 3 summarizes *in vivo* results, presented as the hypocalcemic effect by various sCT administrations in terms of calcium concentration in plasma relative to its initial level. As expected, sCT administered in aqueous dispersion did not show any beneficial effect better than control. Unmodified sCT-loaded PLGA nanoparticles represented hypocalcemic effect similar to the one previously reported [17]. Besides, the plasma calcium concentration returned back to normal level about 10 hours after the drug was administered orally. Hence, a prolonged therapeutic effect was hardly anticipated from the unmodified sCT-loaded PLGA nanoparticles.

The hypocalcemic effect of oral sCT administration was significantly improved by chitosan modifications. They even showed a sustained drug release effect as well. If these two chitosan-modified particles are compared to each other, sCT-PLGA-CHT1 particles seem to show a stronger and longer hypocalcemic effect than

sCT-PLGA-CHT2. All positive points from ANOVA and SNK analysis are shown with an asterisk (*). A separate analysis indicated that the hypocalcemic effect of sCT-PLGA-CHT1 particles is superior to sCT-PLGA particles at almost every time point, whereas they are significantly better than sCT-PLGA-CH2 at many time points.

As mentioned previously, this difference might be associated with the spatial distribution of chitosan molecules in medicated PLGA matrix. When chitosan was deposited mostly on the outermost surface of the PLGA particles as in sCT-PLGA-CHT2, it was more likely to diffuse out during the passage of gastric region. Accordingly, some part of chitosan coating might have been lost away when medicated PLGA particles arrived at the intestinal tract.

In the case of sCT-PLGA-CHT1 particles, the situation would be a little different from above. Since some part of chitosan molecules is believed as embedded in PLGA matrix, its retention rate after gastric passage would be higher than that of sCT-PLGA-CHT2. Hence, a higher proportion of chitosan molecules reached the intestinal wall to take a stronger and longer hypocalcemic effect as shown in Fig. 3. In this context, a better sustained release effect resulted. As well known, chitosan improves drug absorption not only by its bioadhesive behavior, but also by temporary loosening of tight junctions of intestinal epithelium to facilitate the paracellular transport of drug molecules [21].

One thing to note is the mechanism of the embedded structure of chitosan in sCT-PLGA-CHT1 particle. When W/O/W emulsion went through an evaporation process to remove the volatile solvent DCM from the O phase containing PLGA molecules, there would be some chances for the counter-diffusion of chitosan molecules into the empty space created by DCM in the O phase. This phenomenon should be sufficiently plausible because the rate of diffusion is substantive when it takes place in liquid or semi-liquid phase. The substantial counter-diffusion of chitosan during the evaporation process would have resulted in the embedded structure of chitosan in PLGA matrix. For sCT-PLGA-CHT2 particles, however, the one-way diffusion of chitosan into already solid PLGA matrix would hardly occur so that chitosan is mostly deposited on the outermost surface of PLGA particles.

When chitosan was coated on sCT-PLGA particles in 1% chitosan solution, it appears that a significant proportion of sCT diffused out of PLGA particles. In this case, some chitosan might have diffused into the PLGA particles as the counter-diffusion took place. Nevertheless, this case does not seem to be desirable because of a low EE value of sCT.

CONCLUSION

The effects of chitosan modification on the physicochemical properties and *in vivo* behaviors of sCT-PLGA nanoparticles were investigated. The chitosan modification was performed by two different methods. An encapsulation efficiency greater than 50% of sCT into PLGA was achieved regardless of the modification method. Among various chitosan-modified particles, sCT-PLGA-CHT1 nanoparticles performed the best in terms of the short-period hypocalcemic effect and the sustained release effect. Their superior behavior was presumably associated with the embedded structure of chitosan molecules in PLGA matrix that probably resulted from a counter-diffusion of chitosan during the evaporation process of W/O/W emulsion.

ACKNOWLEDGEMENT

This work was supported by the Inje Research and Scholarship Foundation in 2009.

REFERENCES

1. R. Hejazi and M. Amiji, *J. Control. Release*, **89**, 151 (2003).
2. M. M. Issa, M. Koping-Hoggard and P. Artursson, *Drug Discovery Today: Technol*., **2**, 1 (2005).
3. P. Sinswat and P. Tengamnuay, *Int. J. Pharmaceutics*, **257**, 15 (2003).
4. W. Sui, L. Huang, J. Wang and Q. Bo, *Colloid. Surf. B: Biointerf*., **65**, 69 (2008).
5. C. Y. Yu, B. C. Yin, W. Zhang, S. X. Cheng, X. Z. Zhang and R. X. Zhuo, *Colloid. Surf. B: Biointerf.*, **68**, 245 (2009).
6. H. Yamamoto, Y. Kuno, S. Sugimoto, H. Takeuchi and Y. Kawashima, *J. Control. Release*, **102**, 373 (2005).
7. N. Nafee, S. Taetz, M. Schneider, U. F. Schaefer and C. M. Lehr, *Nanomedicine*, **3**, 173 (2007).
8. K. Tahara, T. Sakai, H. Yamamoto, H. Takeuchi and Y. Kawashima, *Int. J. Pharmaceutics*, **354**, 210 (2008).
9. R. Yang, S. G. Yang, W. S. Shim, F. Cui, G. Cheng, I. W. Kim, D. D. Kim, S. J. Chung and C. K. Shim, *J. Pharm. Sci*., **98**, 970 (2009).
10. R. Yang, W. S. Shim, F. D. Cui, G. Cheng, X. Han, Q. R. Jin, D. D. Kim, S. J. Chung and C. K. Shim, *Int. J. Pharmaceutics*, **371**, 142 (2009).
11. M. L. Manca, S. Mourtas, V. Dracopoulos, A. M. Fadda and S. G. Antimisiaris, *Colloid. Surf. B: Biointerf.*, **62**, 220 (2008).
12. M. L. Manca, G. Loy, M. Zaru, A. M. Fadda and S. G. Antimisiaris, *Colloid. Surf. B: Biointerf.*, **67**, 166 (2008).
13. M. Zaru, M. L. Manca, A. M. Fadda and S. G. Antimisiaris, *Colloid. Surf. B: Biointerf.*, **71**, 88 (2009).
14. M. Garcia-Fuentes, C. Prego, D. Torres and M. J. Alonso, *Euro. J. Pharm. Sci*., **25**, 133 (2005).
15. J.-S. Lee, J.-S. Kim and H.-G. Lee, *Colloid. Surf. B: Biointerf.*, **70**, 213 (2009).
16. G. Coppi and V. Iannuccelli, *Int. J. Pharmaceutics*, **367**, 127 (2009).
17. J.-Y. Jang, B.-S. Kwon, H.-E. Lee, J.-S. Kang, S.-K. Lee and G.-J. Choi, *J. Ind. Eng. Chem*., **13**, 1043 (2007).
18. T.-S. Jung, B.-S. Kwon, H.-E. Lee, A.-Y. Kim, M.-J. Lee, C.-R. Park, H.-K. Kang, Y.-D Kim, S.-K. Lee and G.-J. Choi, *Korean J. Chem. Eng*., **26**, 131 (2009).
19. P. K. Smith, *Anal. Biochem*., **159**, 76 (1985).
20. L. A. Kaplan, A. J. Pesce and S. C. Kaczmierczak, Clinical Chemistry: Theory, Analysis, Correlation. 4th Ed., Mosby Inc., St. Louis (2003).
21. C. Prego, M. Garcia, D. Torres and M. J. Alonso, *J. Control. Release*, **101**, 151 (2005).